IBRACON
IBRACON Structures and Materials Journal
Revista IBRACON de Estruturas e Materiais
ISSN 1983-4195 *ismj.org*
SciELO

ORIGINAL ARTICLE

Nonlinear evaluation of reliability-based topology optimization of concrete deep beams

Análise não linear e otimização topológica baseada em confiabilidade de vigas altas de concreto

Rodrigo Reis Amaral[a]
Jorge Luis Palomino Tamayo[a]
Liércio André Isoldi[b]
Herbert Martins Gomes[a]

[a]Universidade Federal do Rio Grande do Sul – UFRGS, Departamento de Engenharia Mecânica, Porto Alegre, RS, Brasil
[b]Universidade Federal do Rio Grande – FURG, Escola de Engenharia, Rio Grande, RS, Brasil

Received 27 September 2024
Revised 15 January 2025
Accepted 15 March 2025

Abstract: Uncertainty has long been a recognized aspect of engineering analysis and design. This inherent unpredictability is typically represented by variability and randomness. In this context, a linear elastic topology optimization (TO) approach with reliability constraints is presented. This method uses an outer loop for the optimization and an inner loop for the reliability analysis. The TO procedure based on the Bidirectional Evolutionary Structural Optimization (BESO) was developed to minimize the structure's concrete compliance and, consequently, reduce the weight for a given reliability index constraint. Failure criterion, such as Ottosen's four-parameter surface is used to check the stress level in the computational domain. Moreover, a nonlinear finite element analysis for the resulting structure is developed in commercial software. The scope here is to conduct a comparative analysis between a reference deep beam from the literature and the optimized topologies to determine the ultimate strength capacity and assess how material reduction affects the failure mode and ultimate load. Results demonstrate resource-efficient and reliable designs with similar structural performance when compared to traditional concrete structures.

Keywords: FORM, UHPFRC, nonlinear analysis, RBDO, Reliability Index Approach.

Resumo: A incerteza tem sido reconhecida há muitos anos como um aspecto importante na análise dos projetos nas engenharias. Essa imprevisibilidade inerente é geralmente representada pela variabilidade e a aleatoriedade. Nesse contexto, é apresentada uma abordagem de otimização topológica (OT) elástica linear com restrição de confiabilidade. Este método utiliza um laço externo para a otimização e um laço interno para a análise de confiabilidade. O procedimento de OT, baseado na Otimização Estrutural Evolutiva Bidirecional, foi desenvolvido para minimizar a flexibilidade da estrutura de concreto e, consequentemente, reduzir o peso, respeitando um índice de confiabilidade estabelecido. Critério de falha, como a superfície de quatro parâmetros de Ottosen, é utilizado para verificar o nível de tensão do domínio computacional. Além disso, é realizada uma análise não linear por elementos finitos da estrutura resultante em um software comercial. O objetivo é realizar uma análise comparativa entre uma viga alta de referência da literatura e as topologias otimizadas, a fim de determinar a capacidade de resistência última e avaliar como a redução de materiais afeta o modo de falha e a carga última. Os resultados demonstram projetos eficientes e confiáveis em termos de recursos, com desempenho estrutural semelhante ao das estruturas tradicionais de concreto.

Palavras-chave: otimização de projeto baseada em confiabilidade, concreto de ultra alto desempenho reforçado com fibras, análise não linear, abordagem do índice de confiabilidade.

Corresponding author: Rodrigo Reis Amaral. E-mail: rodrigo_amaral_23@hotmail.com
Financial support: This study was financed in part by the CAPES (Coordination for the Improvement of Higher Education Personnel) – Finance Code 001. The authors also thank CNPq (Brazilian National Council for Scientific and Technological Development).
Conflict of interest: The authors declare that they have no known competing financial interests or personal relationships that could have appeared to influence the work reported in this paper.
Data Availability: The data, models, and algorithms that support the findings of this study are available from the corresponding author upon reasonable request.

How to cite: R. R. Amaral, J. L. P. Tamayo, L. A. Isoldi, and H. M. Gomes, "Nonlinear evaluation of reliability-based topology optimization of concrete deep beams", *Rev. IBRACON Estrut. Mater.*, vol. 18, no. 3, e18302, 2025, https://doi.org/10.1590/S1983-41952025000300002

1 INTRODUCTION

Most engineering analyses and designs involve uncertainty. Structural response can be highly sensitive to uncertainties in material properties, manufacturing process, external loading conditions, and analytical or numerical modeling. The fundamental challenge is to ensure satisfactory performance given the unpredictability of most design variables. The presence of such uncertainty cannot be entirely eliminated, but with reasonable efforts, its effect on the design values of load effects (such as forces, stresses, deformations, displacements, cracks) can be reasonably reduced to an acceptable level. Since there is always some probability of failure, this observation clearly implies that engineering systems cannot be designed to be "risk free" [1]–[3].

In structural reliability analysis, a "limit state" is defined as a condition to be met. This threshold is typically represented mathematically by a limit state or performance function, which indicates an event that moves the structure from an operational to a non-operational state [3], [4]. According to Farsangi et al. [5], the limit state function can be treated as a probabilistic constraint in reliability-based topology optimization (TO). It is a distinct concept from the objective function, which typically aims to minimize compliance (maximizing stiffness). As long as the limit state function can be expressed in terms of the random variables during the optimization process, there is no restriction on the choice of the limit state function, which is most of the time based on strength criteria.

Avoiding suboptimal or non-optimal designs, which can result from deterministic approaches, is the primary motivation for integrating uncertainty into the TO process. By incorporating stochastic methods that consider the statistical properties of uncertain variables, the optimization process aims to maintain structural reliability and optimize costs. This approach ensures that the resulting topology is robust and resilient to unforeseen events [6]–[8]. One of the earliest papers [9] introduced a novel approach called Reliability-Based Topology Optimization (RBTO), which integrated reliability analysis into traditional topology optimization methods. The main assumptions of the RBTO model include the consideration of randomness in key structural parameters such as geometry and applied loads, which are treated as random variables. The methodology involved coupling reliability analysis with topology optimization through a specific optimization procedure, allowing for the generation of optimal topologies that are more reliable than those produced by deterministic methods. By incorporating reliability constraints, the resulting structures exhibited improved performance under uncertainty while maintaining the same weight as deterministic designs. The findings revealed that the RBTO model not only yields different topologies compared to deterministic optimization but also enhances the volume/reliability ratio of the structures. Additionally, the model demonstrated the capability to produce various topologies based on different target reliability levels, thus offering a strategic advantage in design optimization. Unfortunately, the paper did not focus on RBTO of reinforced concrete structures.

In this context, a linear elastic TO procedure with reliability constraint, defined by a stress limit state function, is applied to a case study of a deep beam with openings. It employs a two-level approach considering probabilistic constraints within the optimization loop. To do this, nested loops can be used: an outer loop for the optimization process and an inner loop for the reliability analysis [10], as in Reliability Index Approach (RIA) for Reliability Based Design Optimization (RBDO) approach. The purpose of the optimization is to maximize the stiffness of the structure while minimizing its weight, based on a predefined reliability index set by the designer. The RIA approach offers the advantage of direct reliability calculation through the reliability index (β), providing clear and interpretable measures of design reliability. It often demonstrates stability in optimization problems compared to the Performance Measure Approach (PMA), although it is more prone to getting stuck in local minima. Additionally, RIA is easier to implement, especially when using gradient-based optimization techniques, and aligns well with traditional design methods familiar to many engineers.

Also, only concrete and voids are considered in this stage of the analysis. The inclusion of steel in the optimization process will be addressed in a future work through a multi-material TO approach (concrete, steel, and voids). A failure criterion such as the Ottosen four-parameter failure surface [11], is used in this stage of the analysis. Lastly, a nonlinear finite element analysis considering material, plasticity, fracture and geometric nonlinearity is conducted in Simulia Abaqus. This final step is to check the ultimate strength capacity and evaluate how material reduction may affect the failure mode of the optimized structures when compared to the reference structure (control structure).

2 LITERATURE REVIEW

Several studies on reliability-based optimization of concrete structures are available in the literature [12]–[14]. Notably, a methodology for the design and reliability evaluation of reinforced concrete structures based on the strut-and-tie model can be found in Pantoja et al. [15]. In this study, the TO procedure is employed with reliability analysis to assist in the design by placing the steel material in the optimum region within the concrete structures. Additionally, a Monte Carlo simulation is used to calculate the reliability index and the failure probability. The results indicate that the compressive strength of concrete has a low impact on the reliability index, with improvements achieved by increasing the steel area. This low sensitivity to the compressive strength can be attributed to the governing failure modes, particularly shear of inclined struts and the yielding of the steel reinforcement (the failure is preceded by large displacements and large strains in steel), which dominate the structural behavior and remain consistent across all analyzed scenarios.

Bobby et al. [16] present a novel framework for the reliability-based TO of dynamically sensitive uncertain building systems subject to stochastic excitation. The method is based on describing the system's reliability through several constraints. These constraints are written in terms of first excursion probabilities posed on the generally non-stationary system response. Results indicated that the proposed method effectively captures the impact of stochastic excitation on the system's reliability, providing robust solutions that enhance the overall safety and performance of the structures.

Siacara et al. [17] focused on the reliability-based design optimization of a concrete dam. This work aimed to determine the minimal dam cross-sectional area and the optimal location for the drainage gallery. Additionally, they ensured adherence to reliability constraints related to overturning, sliding, flotation, and eccentricity failure modes. The optimal placement of the drainage gallery consistently reduced its dimensions across all solutions. Cohesion and friction angle along the dam base interface were important uncertain parameters affecting dam stability.

Recently, an effective reliability-based TO framework for the layout of viscoelastic dampers in energy-dissipating structures under nonstationary seismic excitation was presented in Xian and Su [13]. This framework formulates the optimization problem using the explicit time-domain method developed for stochastic sensitivity analysis of fractionally-damped structures, combined with the adjoint variable method. The optimal layout of fractional viscoelastic dampers is determined using the gradient-based Method of Moving Asymptotes (MMA), with the Solid Isotropic Material with Penalization (SIMP) technique driving the existence variables to binary solutions. The study demonstrates the feasibility of the explicit time-domain method and reliability-based TO framework with a 4-storey building frame structure equipped with fractional viscoelastic dampers. However, the current approach assumes the Poisson process, characterized by statistically independent events occurring at a constant average rate over time, which may introduce errors for narrow-band response processes.

3 THEORETICAL BASIS

The development of Section 3.1 primarily references the works of Ang and Tang [6], Le et al. [18], Huang and Xie [19], Amaral et al. [8], Farsangi et al. [5], and Borges et al. [20].

3.1 Reliability-based Topology Optimization for Maximizing Stiffness with Stress Limit State Function

Probability theory is commonly used to account for uncertainties in load and resistance parameters in Reliability-Based Topology Optimization (RBTO). While there are several ways to formulate an RBTO problem, the general goal is to determine an optimal vector of design variables $\boldsymbol{x}_j = \left(x_{1j}, x_{2j}, \dots, x_{ij}, \dots, x_{Nj}\right)^T$ that minimizes an objective function of interest while satisfying a series of deterministic and probabilistic constraints, where $\boldsymbol{x}_j$ is the design variable vector with N terms (finite elements), x_{ij} is the material density of the i^{th} element of the j^{th} material used in the material interpolation scheme ($x_{ij} = 1$ for $E \geq E_j$ and $x_{ij} = x_{min}$ for $E \leq E_{j+1}$), where E is the elasticity material modulus, where x_{min} is threshold value to identify the less stiff material within the loop. A typical problem for TO minimizing the compliance with reliability constraints can be written as:

$$\begin{aligned} &Find\ \boldsymbol{x}_j = \left(x_{1j}, x_{2j}, \dots, x_{ij}, \dots, x_{Nj}\right)^T \\ &\quad to\ Minimize\ C = \frac{1}{2}\boldsymbol{u}^T\boldsymbol{K}\boldsymbol{u} \\ &Subject\ to: \begin{cases} \beta_k \leq \beta_{target,k}\ k = 1, \dots, m \\ \boldsymbol{K}\boldsymbol{u} = \boldsymbol{f}^{ext} \\ Error(C) < \Theta \end{cases} \end{aligned} \tag{1}$$

where C denotes the compliance, Θ is an allowable convergence tolerance, $\boldsymbol{u}$ is the global displacement vector, $\boldsymbol{K}$ is the global stiffness matrix, $\mathbf{f}^{ext}$ represents the external force vector, N is the number of elements used to discretize the design domain, β_k is the k-th reliability index during the TO process for a constraint k, $\beta_{target,k}$ is the target reliability index stipulated by the designer to be attained.

In Equation 1, voids and concrete must be chosen as the phases to be distributed on the computational domain based on compliance. The goal at this stage is to minimize the structure's compliance (maximizing stiffness) while maintaining a user-specified reliability constraint $\beta_{target,k}$ and, as a result, reducing the volume of material and ensuring, in this way, a reduction in most of the dead load due to the concrete mass removal.

In relation to the TO process, this study considers a density-based model for the modulus of elasticity of materials and account for the structure's weight. These are defined as $E(x_{ij}) = x_{ij}^p E_j + (1 - x_{ij}^p) E_{j+1}$, and $\rho(x_{ij}) = x_{ij}^p \rho_j + (1 - x_{ij}^p) \rho_{j+1}$, where ρ_j is the density of the material and the superscript p is a penalization factor to assure that the current element belongs to one material (phase) only, x_{min} (voids) or close to 1 (plain concrete).

About the elemental sensitivity number, which is used to drive the optimization process, it is defined as the compliance at the elemental level and can be stated as:

$$\alpha_i^e = -\frac{1}{p}\frac{\partial C}{\partial x_i} = \frac{1}{2} x_i^{p-1} \boldsymbol{u}_i^T \boldsymbol{k}_i^0 \boldsymbol{u}_i \tag{2}$$

Concerning the stress constraints to provide tight control on the stress levels owing to the maximum function, the q-norm is employed to smoothly evaluate the stress weights in the elements with an empirical exponent q.

$$\max_{i=1\ldots N}(\sigma_i(\boldsymbol{x})) \cong \left[\sum_{i=1}^{N} \sigma_i(\boldsymbol{x})^q\right]^{1/q} \leq \sigma_{lim} \tag{3}$$

The four-parameter failure surface proposed by Ottosen [11] is employed to check the stress level in the optimized concrete structures. According to Oliveira et al. [21], Ottosen's criterion involves the stress invariants I_1 and J_2 and the loading angle θ_{load} in its equation. Its smoothness, convexity, and curved meridians gradually transition from an almost triangular shape to a nearly circular deviatoric plane as the hydrostatic pressure increases, making this criterion suitable for failure simulation of concrete structures.

The four-parameter model developed by Ottosen [11] is expressed in the form

$$f(I_1, J_2, \cos 3\theta) = c_1 \frac{J_2}{f_c'^2} + \lambda \frac{J_2^{0.5}}{f_c'} + c_2 \frac{I_1}{f_c'} - 1 = 0 \tag{4}$$

where c_1 and c_2 are constants, and λ is a function of $\cos 3\theta$:

$$\lambda = \begin{cases} k_1 \cos\left[\frac{1}{3}\cos^{-1}(k_2 \cos 3\theta)\right] & \text{for } \cos 3\theta \geq 0 \\ k_1 \cos\left[\frac{\pi}{3} - \frac{1}{3}\cos^{-1}(-k_2 \cos 3\theta)\right] & \text{for } \cos 3\theta \leq 0 \end{cases} \tag{5}$$

where $\cos 3\theta = 3\sqrt{3} J_3 / (2\sqrt{J_2^3})$ and k_1 and k_2 are constants defined by CEB-FIP [22], as a function of f_{cm} and f_{tm}. Therefore, the following constants can be defined as: (*i*) $\alpha = 1/(9k^{1/4})$, (*ii*) $\beta = 1/(3.7k^{1.1})$, (*iii*) $c_1 = 1/(0.7k^{0.9})$ and (*iv*) $c_2 = 1 - 6.8(k - 0.07)^2$, and $k = f_{tm}/f_{cm}$. According to Chen and Han [23] the model encompasses several earlier models as special cases, e.g., the von Mises model for $c_1 = c_2 = 0$ and $\lambda =$ constant, and the Drucker-Prager model for $c_1 = 0$ and $\lambda =$ constant.

To ensure smoothness in the TO process, and to avoid checkerboard patterns and mesh dependency, sensitivity filters are typically used. This leads to truss-like members with cross-sections that depend on a local length r_{min}, as defined by:

$$\alpha_i^{Nodes} = \frac{\sum_{j=1}^{nk} \omega(r_{ik}) \alpha_i^e}{\sum_{j=1}^{nk} \omega(r_{ik})} \tag{6}$$

where nk is the number of nodes that are neighbors (at a distance less than or equal to r_{min}) of element i, r_{ik} is the distance between the center of the element i and node k, $\omega(r_{ik})$ are linear weighting factors $\omega(r_{ik}) = r_{min} - r_{ik}$ for $dist\ (i,k) < r_{min}$, and $\omega_{ik} = 0$ in case $dist\ (i,k) \geq r_{min}$, and α_k^{nodes} is the sensitivity of the nodes within the neighborhood radius r_{min} with center at the finite element i.

Regarding the evaluation of the reliability index β, which is used to establish the final shape of the topology, the entire process is an intricate interplay of optimization and reliability analysis, often represented as nested loops in computational terms. The outer loop (TO process) is the initial stage of the process. It is responsible for defining the topology with the objective of maximizing the structural stiffness while minimizing its weight. For each iteration of the outer loop, the inner loop (reliability analysis) is initiated. The inner loop is dedicated to determining the reliability index β for the current topology. This procedure is known as the Reliability Index Approach (RIA, Kim et al. [24],). The First Order Reliability Method (FORM) is employed for this analysis and the main parameter obtained by the method is the reliability index, defined as:

$$\beta = \Phi^{-1}(1 - P_f) \tag{7}$$

where β is the reliability index, representing the boundary between safe and failure states; Φ^{-1} is the inverse of the cumulative distribution function of a standard normal distribution, and P_f is the is the probability of failure of the structural system:

$$P_f = \int_{-\infty}^{\infty} \int_{-\infty}^{s \geq r} f_R(r) f_S(s) dr ds = \int_{-\infty}^{\infty} F_R(\boldsymbol{X}) f_S(\boldsymbol{X}) d\boldsymbol{X} = P[G(\boldsymbol{X}, \boldsymbol{d}) \leq 0] \tag{8}$$

where $f_S(s)$ is the probability density function of the demand loads, $f_R(r)$ is the cumulative probability density function of the resistances, R is the resistance variable, S is the demand variable, $\boldsymbol{X}$ is the vector of random variables, $\boldsymbol{d}$ is the vector of deterministic parameters, and $G(\boldsymbol{x}, \boldsymbol{d})$ is the limit state function. A safety condition is assumed when $G(\boldsymbol{x}, \boldsymbol{d}) > 0$; otherwise, if $G(\boldsymbol{x}, \boldsymbol{d})$ is negative, it is defined as a failure condition.

The FORM optimization problem is then solved to find the shortest distance from the origin to the corresponding point on the limit state surface in the standardized normal space (Most Probable Point, MPP). This distance is the reliability index β, and can be expressed as:

$$\begin{cases} \beta = \min \sqrt{\boldsymbol{U}^{\mathrm{T}} \boldsymbol{U}} = ||\boldsymbol{U}|| \\ Subject\ to\ G(\boldsymbol{X}, \boldsymbol{d}) = 0 \end{cases} \tag{9}$$

where $\boldsymbol{U}$ is the random variable transformed into the standardized normal space, represented by $\boldsymbol{U} = \boldsymbol{L}^{-1}(\boldsymbol{X} - \mu_{eq})$. Here, $\boldsymbol{L}$ is the covariance matrix $\boldsymbol{L} = \mathrm{COV}(\boldsymbol{X}, \boldsymbol{X})$ and μ_{eq} is the equivalent vector of Gaussian mean values.

Therefore, to numerically solve the reliability analysis employing FORM, the iterative equation for the solution of the problem in Equation 9 is employed:

$$\mathbf{U}^{k+1} = [\frac{\left(\frac{\partial G^k}{\partial \mathbf{U}}\right)^T \mathbf{U}^k - \left(\frac{\partial G^k}{\partial \mathbf{U}}\right)^T}{\left(\frac{\partial G^k}{\partial \mathbf{U}}\right)^T \frac{\partial G^k}{\partial \mathbf{U}}}] \left(\frac{\partial G^k}{\partial \mathbf{U}}\right)^T \tag{10}$$

$$\beta^{k+1} = \sqrt{(\mathbf{U}^T)^{k+1}\, \mathbf{U}^{k+1}} \tag{11}$$

where k indicates the current iteration of the reliability analysis.

A stopping criterion for iterations may be formulated based on the convergence of $\mathbf{U}$, β, and $G(\mathbf{X}, \boldsymbol{d}) = 0$. The measure of importance (sensitivity) of each random variable θ to the reliability index β can be evaluated by:

$$\theta = -\frac{\left(\frac{\partial G^k}{\partial \mathbf{U}}\right)^T}{\sqrt{\left(\frac{\partial G^k}{\partial \mathbf{U}}\right)^T \frac{\partial G^k}{\partial \mathbf{U}}}} \tag{12}$$

Considering the main contribution for the MPP to the failure probability, an approximate relation (for linear limit state function) between Failure Probability and the reliability index uses the definition of the standard cumulative distribution function (Φ) and is given by $P_f = \Phi(-\beta) = 1 - \Phi(\beta)$. By incorporating this methodology, the reliability index β is computed for each topology iteration, ensuring that the final design meets the required reliability criteria while optimizing structural performance.

Figure 1 shows a flowchart depicting how the reliability analysis interacts with the deterministic TO, based on the RIA scheme, with two nested loops: the outer loop for the deterministic optimization and the inner loop for the reliability analysis. Design variables $\boldsymbol{d}$ are presented by the vector of densities on the elements $\boldsymbol{x}$, and the random variables $\mathbf{X}$, represented by variables $\mathbf{Z}$ in order not be confused with densities. As usual, the inner loop is presented in FORM, First Order Reliability Analysis, for the reliability index β evaluation.

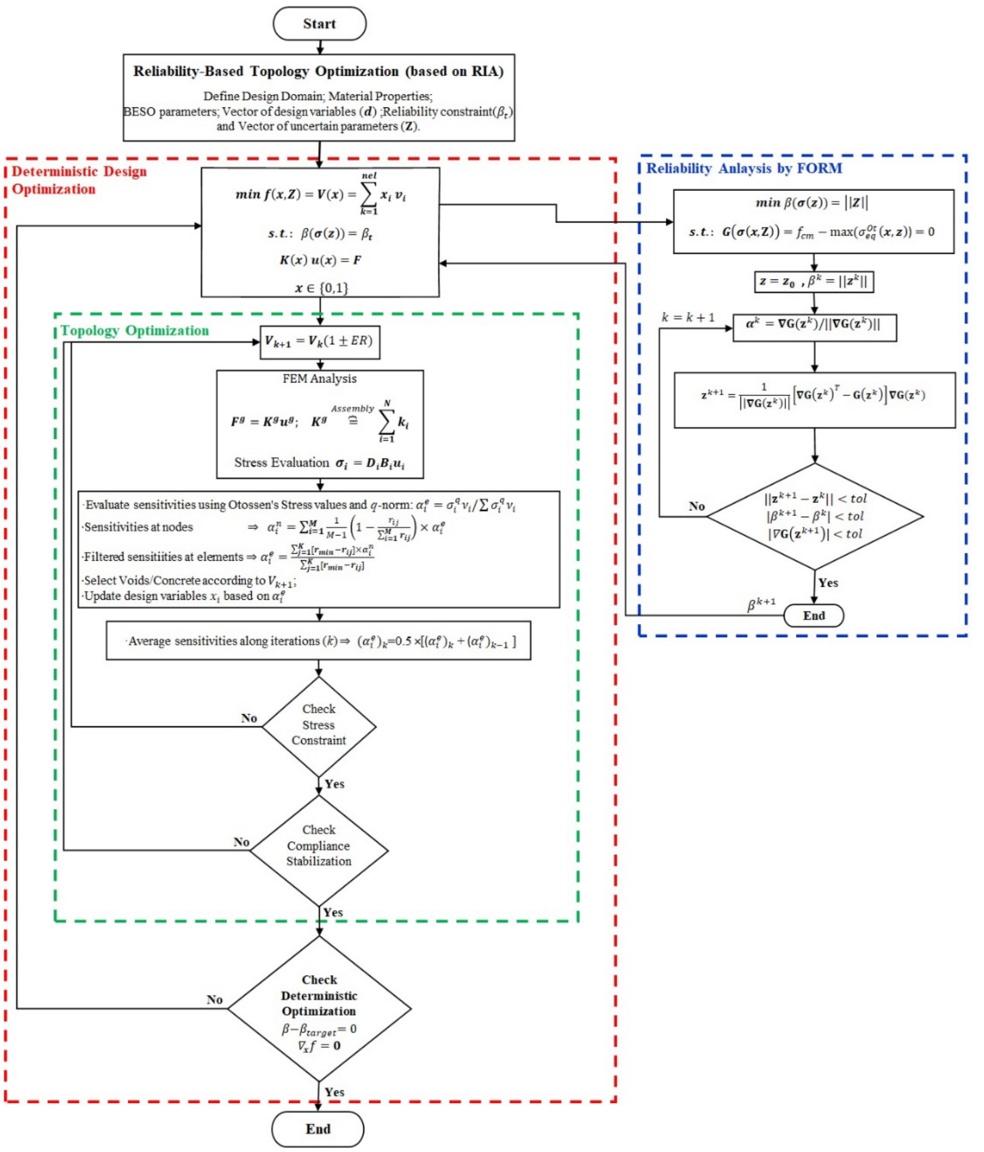

Figure 1. Flowchart for the Reliability-based Topology Optimization implemented in this paper.

4 RESULTS AND DISCUSSIONS

The design based on the Strut-and-Tie (STM) Method of a continuous deep beam with a width of 80 mm, a height of 400 mm, and a length of 1900 mm is used to perform the TO process with reliability constraints. This continuous deep beam is made of an ultra-high-performance fiber-reinforced concrete (UHPFRC). Experimental data from Yousef et al. [25], shown in Figure 2, provided the basis for the selected structure for the TO process and the development of the numerical analysis presented in this paper. Steel reinforcement is not considered in this comparison between the optimized and the reference structures. Figure 2 only displays the specimen's geometry and boundary conditions.

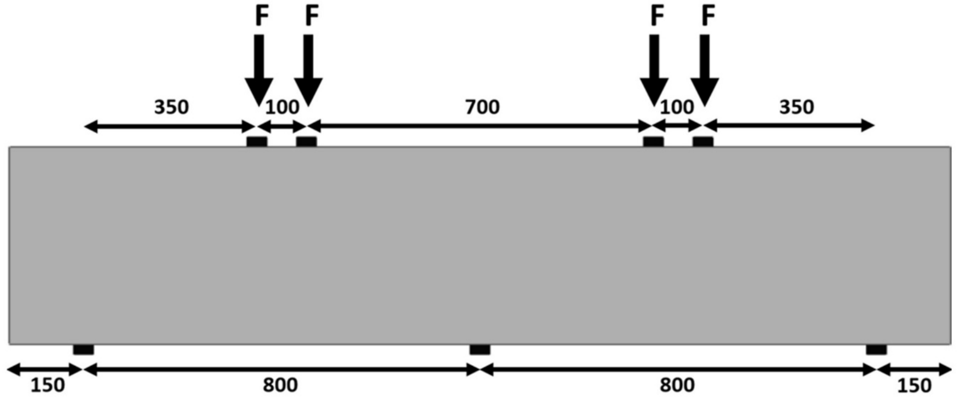

Figure 2. Continuous deep-beam geometry. Units in mm.

The theoretical load capacity was not reported in Yousef et al. [25]. This data is required to determine the reliability index of the structure presented in Figure 2 during the iterative process of removing material from regions with high compliance during the TO process in MATLAB. But the problem provides the amount of steel used in the tie region (1520.53 mm^2), and the yield strength of the steel f_{yk} (426.3 MPa). So, the design load was determined using the declared area of the main reinforcement, which is related to the reaction force by the equation $A_s = (F/f_{yd})$, resulting in a design load of 563.65 kN. As only the concrete material is considered in the optimization process, a reduced load of 193.755 kN (35% of the design load) is assumed. This reduction is applied to account for the absence of steel reinforcement in the analysis and to ensure that the loading conditions reflect the behavior of the concrete alone. The load is distributed across four steel plates, each measuring 40 × 80 mm and a thickness of 20 mm.

For characterization of the material properties, specimens were molded for the determination of the mechanical properties of the UHPFRC. The UHPFRC mix consists of 900 g of Portland cement (grade 52.5N), 225 g of silica fume, 775 g of sand, 270 g of quartz powder, 168 g of water, and 36 g of superplasticizer. Additionally, the mix includes 117 g of end-hooked steel fibers with a diameter of 0.2 mm, representing 1.5% of the total volume. This resulted in a mean compressive strength f_{cm} of 143.50 MPa, splitting tensile strength (or diametral compression strength) f_{tm} of 10.50 MPa, and a modulus of elasticity E_c of 44,766.08 MPa.

The TO process developed in MATLAB still requires defining some parameters. The properties of the concrete obtained from the experimental data of Yousef et al. [25] are already defined, except for the Poisson's ratio ν_c and mass density ρ_c, which were not reported and were set to 0.2 and 2530 kg/m^3, respectively. It is also assumed that the voids have values close to zero (0.0001) for both Young's modulus E_v and Poisson's ratio ν_v. Table 1 provides the remaining parameters required for the software. It is important to emphasize that the analysis performed in MATLAB involves a 2D plane stress analysis.

Table 1. BESO parameters adopted for the optimization of the continuous deep beam.

$N_x \times N_y$ (Finite Elements)	$d_x^e = d_y^e$ (m)	ER (%)	r_{min} (m)	p	q	μ
380×80	0.005	1.0	0.125	3	4	0.5

In Table 1, N_x and N_y represents the number of finite elements in the x and y directions, respectively; d_x^e and d_y^e are the size of the side of the finite element in the x and y directions, respectively. The evolutive ratio (ER) indicates the rate at which concrete volume is removed from the computational domain in each iteration. The filter length scale (r_{min}) is designed to avoid checkerboard patterns and mesh dependency. The penalization factor (p) has been previously explained, and the degree of stress proportion (q) to define the maximum stress follows Le et al. [18]. Lastly, the moment factor (μ) for stabilizing the TO algorithm is detailed in Huang and Xie [19].

About the reliability analysis, a stress limit state function is defined as $g(\boldsymbol{X}) = f_{cm} - \max(\sigma_{eq}^{Ot}(\boldsymbol{x}))$, where f_{cm} is the compressive strength of the concrete and σ_{eq}^{Ot} is the equivalent stress of Ottosen. Here, the max of the function assures that any point in the deep beam is considered in the constraint equation. Six variables are chosen as random variables based on observed experimental variability and experimental data. The distribution type, mean values, and standard deviation for each of these random variables are: (i) the compressive strength of the concrete f_{cm} (MPa) N:(143.50; 21.525) , (ii) the Young's modulus E_c (MPa) N:(44,766.08; 6,714.912), (iii) the applied vertical load F(kN) N:(193.755; 38.751), (iv) the beam's span L (mm), N: (1900; 57) (v) beam's height h (mm), N: (400; 12), and (vi) beam's width b_w (mm), N: (80; 2.4). The vector of random variables is defined as $\boldsymbol{X} = (\mathrm{f_{cm}}, E, F, L, \mathrm{h}, b_w)^T$.

The assumption for normal distribution was based on the fact that it is suitable for modeling parameters like the Young's modulus of concrete, loads, dimensions, and concrete strength, due to its mathematical properties and practical convenience. Based on the Central Limit Theorem (CLT), when multiple independent factors influence a parameter, their combined effect tends to produce a normal distribution. For instance, in concrete testing, variations in material properties and environmental conditions often lead to approximately normally distributed results. The normal distribution simplifies statistical analysis, as it is fully characterized by just its mean and standard deviation, allowing engineers to easily assess variability and design for safety using well-understood methods. However, relying on the normal distribution can introduce errors if the data does not actually follow a normal distribution. For example, concrete strength and other material properties may exhibit skewness or a log-normal distribution, especially when the data contains a few extreme values or outliers. In such cases, assuming normality could lead to misleading conclusions, such as overestimating the probability of extreme events or failing to account for certain risks. In this paper, this hypothesis was assumed based on generally accepted literature [26]. Thus, the results of the optimized structure with reliability index β_{target} of 3.3, 4.2, and 4.4 are illustrated in Figures 3 and 4.

The JCSS Probabilistic Model Code [27], as specified in ISO 2394-15 [28], is used for the target chosen values. This code provides target reliabilities for different classes of structures, with an emphasis on economic optimization. For this study, class 3 is relevant, representing most residential buildings, typical bridges and tunnels, typical offshore facilities, and larger or hazardous industrial facilities.

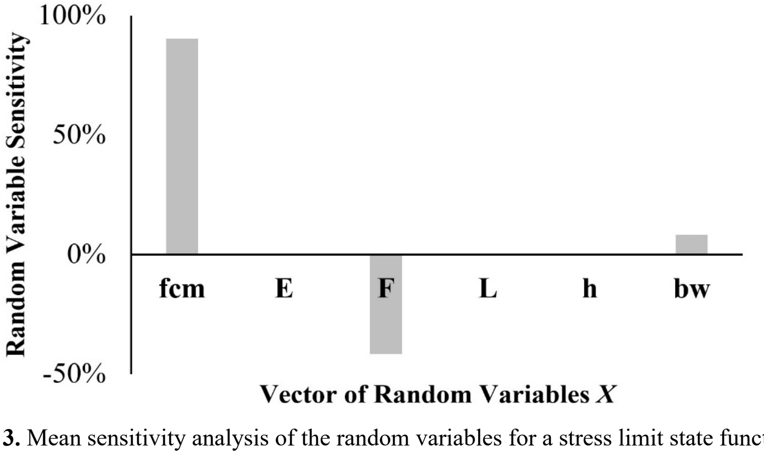

Figure 3. Mean sensitivity analysis of the random variables for a stress limit state function.

According to the sensitivity analysis shown in Figure 3, the highest sensitivity variable of all analyzed topologies is the compressive strength of the concrete $(\theta_1 = +0.90)$. This indicates that an increase in this variable leads to a significant positive sensitivity in the reliability index β. Also, the magnitude of the load $(\theta_3 = -0.41)$ exhibits a considerable negative sensitivity. The negative value of θ_3 implies that an increase in the load magnitude inversely affects the reliability index β, thereby jeopardizing the structural integrity. Regarding Young's modulus (θ_2), no significant influence was captured for this variable when considering a stress limit state function. This indicates that variations in Young's modulus do not substantially affect the reliability index under a stress constraint. However, if a displacement limit state function were considered, this variable would play a major role since it directly influences how much the structure deforms.

Regarding the influence of the stochastic variables related to the beam's dimensions – θ_4 (span), θ_5 (height), and θ_6 (width) – it was observed that these variables exhibited minimal or no influence on the sensitivity analysis when considering a stress limit state function. This outcome can be attributed to several factors: (i) the influence of θ_4 on local stress concentrations might be negligible because the span primarily affects the global behavior of the structure, while local stress concentrations are more influenced by material properties, load magnitude, and geometric discontinuities; and (ii) θ_5 and θ_6 are crucial for determining the moment of inertia, which affects the bending resistance. However, according to Amaral et al. [8], θ_5 and θ_6 appear to have no significant effect on the optimized beam topologies, likely because the optimization process inherently adjusts the design to mitigate the impact of these dimensions on the stress distribution.

Table 2 shows the resulting topologies that satisfy the reliability constraint and the mechanical behavior (strength and stiffness) when evaluated under a stress limit state function. It should be mentioned that these results were obtained without considering magnification coefficients for loads and reduction coefficients for material strength during the optimization process. As it can be seen, all topologies present a stress level far below the compressive strength of the concrete (143.50 MPa), which indicates a safety factor of 2.64, 3.36, and 3.68 for the topologies with a reliability index β of 3.3, 4.2, and 4.4, respectively. The safety factor is a measure of the structural capacity to withstand loads beyond the expected maximum load, calculated as the ratio of the concrete's compressive strength to the actual stress level experienced by the structure. Additionally, it was possible to achieve a material reduction ranging from 44.30% ($\beta =$ 3.3) to 29% ($\beta = 4.4$). The material reduction is calculated by subtracting the final volume $V_{f\,conc}$ achieved through the optimization process from the initial volume (100%) for a given reliability constraint β.

In the stiffness analysis of the optimized structures, the maximum deflection δ_{max} is just below the region of load application. According to ACI 318-19 [29], it is a value below the maximum deflection allowed for beams, which shall not exceed 1/325 of the span (5.85 mm for a span of 1900 mm). Allowable deflection limits are critical to ensure beams' structural integrity and serviceability, as exceeding these limits could lead to visible cracking or even failure.

Topology	Probability of Failure P_f	$V_{f\,conc}$ [%]	C [Nm]	δ_{max} [m]	σ_{max}^{0t} [MPa]
 $\beta = 3.3$	5.089×10^{-4}	55.70	2.768	-6.68×10^{-5}	54.04
 $\beta = 4.2$	1.091×10^{-5}	67.50	2.348	-5.62×10^{-5}	42.76
 $\beta = 4.4$	5.768×10^{-6}	71.00	2.264	-5.41×10^{-5}	39.02

Figure 4. Mechanical and reliability results for optimized continuous deep beams.

Lastly, a qualitative analysis of the mechanical behavior and crack patterns of the three optimized structures is presented in Figure 4, and the reference structure is presented in Figure 2. The Concrete Damaged Plasticity (CDP) model from Abaqus is used to capture the nonlinearity of the concrete in this final analysis. There are specific inputs to the CDP related to the plasticity model that are specific to the concrete used. Table 2 shows the plasticity parameters used for the analysis.

Table 2. CDP plasticity parameters.

Dilation angle ψ (°)	Eccentricity ϵ	f_{b0}/f_{c0}	K_c	Viscosity parameter η
25	0.1	1.16	0.6667	0

Furthermore, an experimental axial compressive and tensile stress-strain relationship for the UHPFRC, developed by Emad et al. [30], is utilized to accurately describe its behavior in the computational domain (see Figure 5). In these entries, the user has to specify the stress and the inelastic strain given $\varepsilon^{inel} = \varepsilon - \varepsilon^{elast}$ where $\varepsilon^{inel} \leq 0$ is considered linear elastic. Regarding the compressive and tensile damage parameters, the user must provide the stress and its plastic strain in the softening phase of the concrete, given by $\varepsilon^{plast} = \varepsilon^{inel} - [d/(1-d)] \times (\sigma/E_c)$, where the damage d (Figure 6) is calculated as $d = 1 - (\sigma/f_u)$, σ is the nominal stress acting at the sampling point, which may be associated to a purely compressive ($\sigma = \sigma_c$) or tensile ($\sigma = \sigma_t$) state, and f_u is the associated ultimate strength related to that state [31].

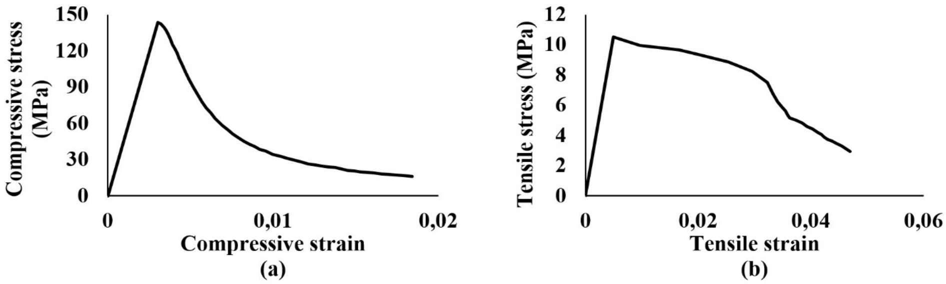

Figure 5. Uniaxial stress-strain relationship for the UHPFRC in (a) compression and (b) tension.

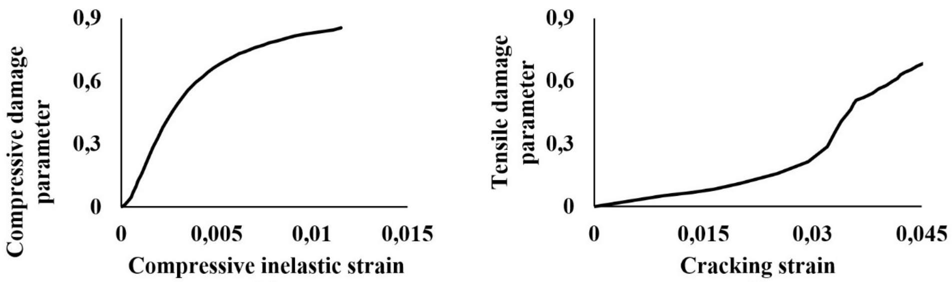

Figure 6. Damage parameter-strain relationship for the UHPFRC in (a) compression and (b) tension.

Regarding the finite element mesh used to discretize the design domain, it was employed for the reference structure a finite element mesh of 17520 C3D8 elements, 15920 C3D8 elements for the topology with $\beta = 4.4$, 14285 C3D8 elements for the topology with $\beta = 4.2$, and 11840 C3D8 elements for the topology with $\beta = 3.3$. The chosen meshes result from a mesh convergence study to ensure the accuracy of the analysis.

Figure 7 presents the results of the analyzed structures by the force-displacement curve. These curves were generated by summing the reaction forces at the supports to determine the total force. To ensure fair comparisons, the total displacement was measured at the bottom part of the deep beam (between loads), as the optimized structure loses volume near the supports.

All optimized structures have decreased stiffness when compared to the reference design, as depicted in Figure 7. Increased displacement and deformability under the same applied force tend to be the outcomes of material reduction. It is also worth emphasizing that topologies IV ($\beta = 3.3$) and III ($\beta = 4.2$) are more likely to fail due to shear forces than tensile or compressive forces caused by bending. The most plausible explanation for this phenomenon is the material distribution during the optimization process that minimizes compliance. This implies that the TO process may result in regions within the structure where shear forces are not adequately accommodated, particularly in locations with abrupt changes or discontinuities in the geometry.

Conversely, Topology II ($\beta = 3.3$) exhibited a similar mechanical behavior to the reference structure, as depicted in Figure 7. This suggests that Topology II exhibits a structural response more akin to traditional concrete structures, and provides a superior load-carrying capacity compared to the other topologies analyzed in this study. It is also noteworthy that a reduction in volume fraction of around 30% for a deep beam may represent a critical threshold. This mechanism of failure is desirable since it provides visual warnings prior to collapse, thus permitting maintenance and repair to prevent a sudden structural failure. As material is removed during optimization, the failure mode shifts from shear to mixed tension-shear failure, compromising the overall performance. The formation of slender regions near the supports and stresses in the D-regions significantly influences the ultimate load, which is governed by shear failure.

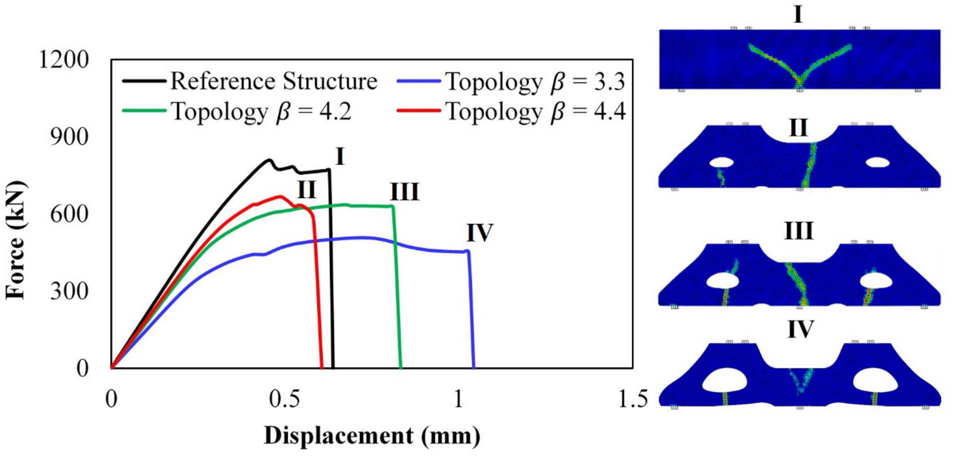

Figure 7. Force-displacement curve for the deep beam and the topologies.

Here, a parallel analysis can be traced with the work of Tamimi et al. [32] where the reliability of reinforced concrete deep beams could be significantly enhanced using optimized STMs and probabilistic analysis. The study involved designing twelve RC deep beams with both standard and optimized STM layouts, followed by a sensitivity analysis using Sobol's method to identify key variables influencing ultimate load capacity. The numerical methods employed include the development of a validated FE model using ABAQUS, which was compared against experimental data from existing literature to ensure accuracy. The analysis reveals that the reliability index ranges from 0.2 to 5.6, depending on the specific STM design and its corresponding load path. Notably, the highest reliability index is observed in beams designed with the L layout, which has the lowest load path Z of 7.73. Conversely, the reliability of the optimized STM layouts falls below a target index of 4 in a particular case, indicating the need for appropriate resistance factors in the design process to maintain safety standards.

5 CONCLUSIONS

A comparative nonlinear evaluation of UHPFRC topologies obtained using a linear TO procedure based on BESO with reliability constraints was presented in this study. In the optimization process, a limit state function based on the stress level ($g(\boldsymbol{X}) = f_{cm} - \max\,(\sigma_{eq}^{Ot}(\boldsymbol{x}))$) was adopted to define the reliability index β as material is removed from the computational domain. To evaluate the reliability of the topologies, the FORM was utilized, incorporating uncertainties in material properties, load magnitude, and the dimensions of the design problem. Additionally, a sensitivity analysis of the stochastic variables was conducted to evaluate their impact on the optimization results.

A normative standard for reliability analysis, ISO 2394-15 [28], was used as a reference to determine the target reliability index β during the optimization process. In this study, Class 3 was adopted to determine the final reliability index since it is relevant to most residential buildings. As a result, the optimization achieved topologies with material reductions ranging from 44.30% to 29%, and safety factors between 2.64 and 3.68. Furthermore, in this initial analysis performed using MATLAB, all topologies met the code requirements for both the ultimate limit state (stress) and the serviceability limit state (stiffness).

Lastly, Abaqus' CDP model was used to incorporate all the material nonlinearities (cracking and fracturing) to accurately identify the failure modes and ultimate loads of the optimized structures. The study indicates that reducing the volume of concrete by about 30% serves as the threshold for the structure to exhibit a structural response that is similar to the behavior of the traditional structure (STM). Over that range, the structure is hypothesized to fail under shear/compression forces rather than tensile/compression forces generated by the bending over the truss-like formed structure. The failure mode transition occurs as a result of the reduced volume. This affects the shear strength due to abrupt geometry changes in the TO process. The formation of slender regions near the supports and stresses in the D-regions significantly influence the ultimate load, which is governed by the shear failure.

REFERENCES

[1] Y. Tsompanakis, N. D. Lagaros, and M. Papadrakakis, *Structural Design Optimization Considering Uncertainties.* London: Taylor & Francis, 2008. http://doi.org/10.1201/b10995.

[2] P. Samui, D. T. Bui, S. Chakraborty, and R. C. Deo, *Handbook of Probabilistic Models.* Amsterdam: Butterworth-Heinemann, 2020.

[3] V. Raizer and I. Elishakoff, *Philosophies of Structural Safety and Reliability.* Boca Raton: CRC Press, 2022. http://doi.org/10.1201/9781003265993.

[4] S. Nowak and K. R. Collins, *Reliability of Structures*. Boca Raton: CRC Press, 2013.

[5] E. N. Farsangi, M. Noori, P. Gardoni, I. Takewaki, H. Varum, and A. Bogdanovic, *Reliability-Based Analysis and Design of Structures and Infrastructure*. Boca Raton: CRC Press, 2022.

[6] H. S. Ang and W. H. Tang, *Probability Concepts in Engineering: Emphasis on Applications to Civil and Environmental Engineering*, 2nd ed. New Delhi: Wiley, 2006.

[7] S.-K. Choi, R. V. Grandhi, and R. A. Canfield, *Reliability-Based Structural Design.* London: Springer, 2007.

[8] R. R. Amaral, J. A. Borges, and H. M. Gomes, "Proportional topology optimization under reliability-based constraints," *J. Appl. Comput. Mech.*, vol. 8, no. 1, pp. 319–330, Jan 2022, http://doi.org/10.22055/JACM.2021.38440.3226.

[9] G. Kharmanda, N. Olhoff, A. Mohamed, and M. Lemaire, "Reliability-based topology optimization," *Struct. Multidiscipl. Optim.*, vol. 26, no. 5, pp. 295–307, 2004, http://doi.org/10.1007/s00158-003-0322-7.

[10] C. López, A. Baldomir, and S. Hernández, “Some applications of reliability-based design optimization in engineering structures,” in *Proc. Int. Conf. High Perform. Optimum Design Struct. Mater.*, Edinburgh, UK, 2014, http://doi.org/10.2495/HPSM140371.

[11] N. S. Ottosen, "A failure criterion for concrete," *J. Eng. Mech. Div.*, vol. 103, no. 4, pp. 527–535, Jun 1977, http://doi.org/10.1061/JMCEA3.0002248.

[12] R. S. Correia, G. F. F. Bono, and C. M. Paliga, "Evaluation of the reliability of optimized reinforced concrete beams," *Rev. IBRACON Estrut. Mater.*, vol. 15, no. 4, e15409, 2022., http://doi.org/10.1590/s1983-41952022000400009.

[13] J. Xian and C. Su, "Reliability-based topology optimization of fractionally-damped structures under nonstationary random excitation," *Eng. Struct.*, vol. 297, pp. 116956, Sep 2023, http://doi.org/10.1016/j.engstruct.2023.116956.

[14] T. Golecki, F. Gomez, J. Carrion, and B. F. Spencer Jr., "Bridge topology optimization considering stochastic moving traffic," *Eng. Struct.*, vol. 292, pp. 116498, Jul 2023, http://doi.org/10.1016/j.engstruct.2023.116498.

[15] J. C. Pantoja, L. E. Vaz, and L. F. Martha, "A reliability criterion to evaluate the performance of strut-and-tie models applied in design and analysis of reinforced concrete structures," *Mecán. Comput.*, vol. XXIX, pp. 9005–9021, 2010.

[16] S. Bobby, A. Suksuwan, S. M. J. Spence, and A. Kareem, "Reliability-based topology optimization of uncertain building systems subject to stochastic excitation," *Struct. Saf.*, vol. 66, pp. 1–16, Mar 2017, http://doi.org/10.1016/j.strusafe.2017.01.005.

[17] A. T. Siacara, G. P. Pellizzer, A. T. Beck, and M. M. Futai, "Reliability-based design optimization of a concrete dam," *Rev. IBRACON Estrut. Mater.*, vol. 15, no. 5, e15501, 2022, http://doi.org/10.1590/s1983-41952022000500001.

[18] C. Le, J. Norato, T. Bruns, C. Ha, and D. Tortorelli, "Stress-based topology optimization for continua," *Struct. Multidiscipl. Optim.*, vol. 41, no. 4, pp. 605–620, 2010, http://doi.org/10.1007/s00158-009-0440-y.

[19] X. Huang and Y. M. Xie, *Evolutionary Topology Optimization of Continuum Structures: Methods and Applications.* Chichester: Wiley, 2010, http://doi.org/10.1002/9780470689486.

[20] J. A. Borges, R. R. Amaral, L. A. Isoldi, W. J. P. Casas, and H. M. Gomes, "A novel BESO methodology for topology optimization of reinforced concrete structures: a two-loop approach," *J. Appl. Comput. Mech.*, vol. 9, pp. 498–512, Feb 2023, http://doi.org/10.22055/jacm.2022.41708.3799.

[21] D. B. Oliveira, S. S. Penna, and R. L. S. Pitangueira, "Elastoplastic constitutive modeling for concrete: a theoretical and computational approach," *Rev. IBRACON Estrut. Mater.*, vol. 13, no. 1, pp. 171–182, Jan 2020, http://doi.org/10.1590/s1983-41952020000100012.

[22] International Federation for Structural Concrete, *CEB-FIP, Model Code 1990: Design Code.* London: Thomas Telford, 1993.

[23] H. Chen and D. J. Han, *Plasticity for Structural Engineers.* New York: Springer, 1988.

[24] S.-R. Kim, J.-Y. Park, W.-G. Lee, J.-S. Yu, and S. Y. Han, "Reliability-based topology optimization based on evolutionary structural optimization," *Int. Schol. Sci. Res. Innov.*, vol. 1, no. 8, 2007, http://doi.org/10.5281/zenodo.1077565.

[25] A. M. Yousef, A. M. Tahwia, and M. S. Al-Enezi, "Experimental and numerical study of UHPFRC continuous deep beams with openings," *Buildings*, vol. 13, no. 7, pp. 1723, 2023, http://doi.org/10.3390/buildings13071723.

[26] M. A. El-Reedy, *Reinforced Concrete Structural Reliability*. Boca Raton: CRC Press, 2012, 376 p.

[27] Joint Committee of Structural Safety, *Probabilistic Model Code: Part 1 - Basis of Design*, 2001. [Online]. Available: www.jcss.byg.dtu.dk/Publications/Probabilistic_Model_Code.aspx

[28] International Organization for Standardization, *General Principles on Reliability for Structures*, ISO 2394-15, 2015.

[29] American Concrete Institute, *Building Code Requirements for Reinforced Concrete and Commentary*, ACI 318-19, 2019.

[30] W. Emad et al., "Metamodel techniques to estimate the compressive strength of UHPFRC using various mix proportions and a high range of curing temperatures," *Constr. Build. Mater.*, vol. 349, pp. 128737, Sep 2022, http://doi.org/10.1016/j.conbuildmat.2022.128737.

[31] M. Smith, *ABAQUS/Standard User's Manual, Version 6.9.* Rhode Island: Dassault Systèmes Simulia Corp., 2009.

[32] M. F. Tamimi, A. A. Alshannaq, and M. I. Abu Qamar, "Enhancing reliability in reinforced concrete deep beams through probabilistic analysis and topology optimized strut-and-tie models," *Structures*, vol. 70, pp. 107872, 2024, http://doi.org/10.1016/j.istruc.2024.107872.

Author contributions: RRA: Conceptualization, Methodology, Software, Validation, Formal analysis, Investigation, Writing - Original Draft, Visualization. JLPT: Validation, Writing - Review & Editing, Visualization, Supervision. LAI: Writing - Review & Editing, Visualization, Supervision. HMG: Conceptualization, Methodology, Software, Formal analysis, Resources, Data Curation, Writing - Review & Editing, Supervision, Project administration, Funding acquisition.

Editors: Sergio Hampshire C. Santos, Daniel Carlos Taissum Cardoso.